ACS OMEGA

Open Access

http://pubs.acs.org/journal/acsodf

Article

Effects of Long-Acting Anticoagulant Rodenticides on Rabbit Plasma Extracellular Vesicles

Intakhar Ahmad, Ruth N. Muchiri, Richard B. van Breemen, Israel Rubinstein, Matthew Lindeblad, and Douglas L. Feinstein*

Cite This: *ACS Omega* 2025, 10, 16410−16418

Read Online

ACCESS | Metrics & More | Article Recommendations

ABSTRACT: Environmental toxicants and physiological stressors can significantly impact the production and composition of extracellular vesicles (EVs), which are mediators of long-distance intercellular communication. Understanding these processes is essential since EVs can exert far-reaching effects on diverse tissues and organs, including the central nervous system, by crossing the blood−brain barrier. This study investigated plasma EV dynamics in response to long-acting anticoagulant rodenticides (LAARs), warfarin analogs with long biological half-lives used to eradicate rodent infestation that also present a public health hazard. EVs were isolated from plasma samples collected from adult male New Zealand White rabbits administered a mixture of 3 potent LAARs (brodifacoum, BDF; difenacoum, DFC; and bromadiolone, BDL) using a polymer-based precipitation technique. Nanoparticle tracking analysis (NTA) revealed a time-dependent decrease in EV concentration and changes in size distribution. Cotreatment of rabbits with the bile sequestrant cholestyramine (CSA), which accelerates LAAR clearance from rabbits, reversed some effects of LAARs on the EVs. Mass spectrometric analysis showed that all 3 LAARs are associated with isolated EVs and that those levels were reduced by CSA. Application of EVs from LAAR-treated rabbits induced microglial cell death. Collectively, our findings suggest that LAARs can influence both the concentration and size distribution of circulating EVs, which in turn may facilitate the transport of LAARs throughout the body where they can have toxic effects.

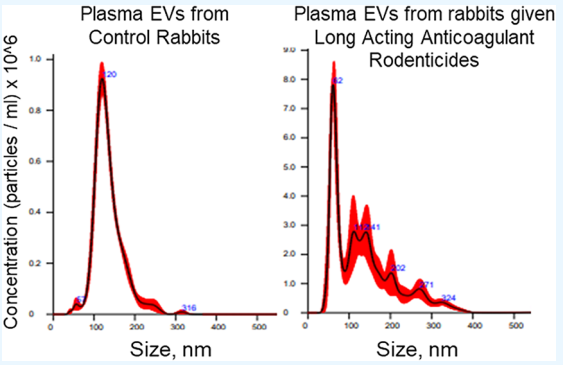

INTRODUCTION

Extracellular vesicles (EVs), including exosomes, are nanometer-sized membrane-bound carriers that facilitate intercellular communication in various biological systems. These versatile vesicles play crucial roles in numerous physiological and pathological processes by transferring nucleic acids, proteins, lipids, and metabolites between cells, thereby modulating the functional state of recipient cells.[1,2] EVs are ubiquitously secreted by nearly all cell types and can be found in diverse bodily fluids, underscoring their potential as biomarkers.[3,4] Moreover, EVs can be engineered as drug delivery vehicles to transport therapeutic agents directly to target cells, highlighting their promise in biotechnology and medicine.[5] However, this capacity raises concerns about their potential to transport harmful cargo and release it into the recipient cell's cytoplasm. Several studies have highlighted the role of EVs in transporting bacterial toxins[6,7] and their involvement in pathogenicity through the delivery of toxin-loaded vesicles to target cells.[8,9] These findings suggest the potential role of EVs in transporting environmental toxins and pesticides. For instance, there are structural similarities between vitamin K epoxide reductase component 1 (VKORC1), the human protein target of the widely used anticoagulant warfarin, and a bacterial molecule crucial for the growth of *Mycobacterium tuberculosis*,[10] suggesting that VKOR or molecules associated with VKORC1 could be present in EVs.

Long-acting anticoagulant rodenticides (LAARs) are warfarin analogs with increased potency to inhibit coagulation by blocking the resynthesis of vitamin K1 (VK1), a necessary cofactor for activation of several clotting factors.[11] In contrast to warfarin, LAARs have biological half-lives on the order of weeks rather than hours due to limited metabolism, as well as undergoing enterohepatic recirculation.[12] LAARs are used throughout the world to reduce rodent infestations by causing internal hemorrhage and death. Due to their long half-lives, LAARs remain active for extended periods, increasing the risk

Received: December 3, 2024
Revised: February 27, 2025
Accepted: April 4, 2025
Published: April 16, 2025

of exposure to nontarget wildlife through bioaccumulation and biomagnification in the food chain.[13] LAARs pose significant risks to birds of prey, mammals, and other wildlife that may ingest poisoned rodents or be directly exposed.[14] Additionally, LAARs can contaminate soil and water sources following aerial dispersal or due to accidental leakage,[15,16] leading to broader ecological consequences and potential human health risks.

We previously showed that administration of brodifacoum (BDF), one of the more potent LAARs, to adult rabbits, causes rapid anticoagulation leading to death, which can be minimized by treatment with cholestyramine (CSA), a bile sequestrant that blocks enterohepatic recirculation and increases LAAR clearance from the body.[17,18] In addition to its anticoagulant actions, BDF also has VK1-independent effects, including induction of kidney damage[19] and neuropathology,[20] and can directly interact with cell membranes to cause cell death.[21]

Whether exposure to LAARs modifies the EV properties has not been examined. However, it has been reported that EVs isolated from patients taking the anticoagulant rivaroxaban, a direct factor Xa inhibitor, differ from those taken from warfarin-treated patients,[22] and the warfarin-treated patients showed an increased inflammatory state, suggesting that reducing VK can exacerbate pathology.[23] It has also been shown that EVs have procoagulative properties, which could influence the degree of anticoagulation induced by LAARs. Several coagulation factors, including tissue factor (TF), an initiator of coagulation, are associated with EVs.[24] Various bodily fluids can initiate coagulation, and this is speculated to be due to the presence of EVs that contain tenase complexes, which comprise tissue factor and activated coagulation factor VII.[25,26] EVs can also express procoagulant signaling factors on their surface, such as phosphatidyl serine (PS).[27] PS normally has an intracellular location, but when exposed due to cellular damage or when on the outer surface of EVs, it can bind to and activate coagulation factors and initiate clotting.[28]

In view of the above, and since numerous biological actions are regulated by EVs,[29] we hypothesized that LAARs might also modify EV properties. In the current study, we show that EVs isolated from LAAR-poisoned rabbits show changes in numbers and size distribution—changes that were reduced by CSA. Furthermore, we demonstrate that LAARs are associated with isolated EVs and can induce cell death in primary microglial cells, suggesting a novel mechanism by which LAARs could be transported throughout the body, causing cell injury and death in vital organs.

MATERIALS AND METHODS

Animals and Treatments. Plasma was obtained as previously described[18] from groups of New Zealand White (NZW) rabbits that had been administered LAARs, alone or with daily treatment of the bile sequestrant CSA. In brief, 2-month-old male NZW rabbits in Group 1 were administered a single bolus dose by gavage of a mixture of three LAARs: brodifacoum (BDF, at a final dose of 200 μg/kg), difenacoum (DFC at a final dose of 800 μg/kg), and bromadiolone (BDL at a final dose of 1.75 mg/kg) based on doses reported for mice[30] and rats.[31] To prevent mortality, vitamin K1 (VK1) was administered daily to all rabbits (5 mg/kg of s.c.). Group 2 rabbits were also administered the bile sequestrant cholestyramine (CSA, 0.67 g/kg, oral gavage) beginning 1 day after LAARs and 30 min before VK1 and continued daily for 10 days. Control Group 3 rabbits consisted of naive controls. All animal procedures were approved by the local UIC IACUC Committee.

Plasma Sample Preparation. Blood samples were collected from the lateral ear vein at days 2, 3, and 10 after LAAR administration. Blood aliquots were collected into heparin BD Vacutainer Tubes (BD Biosciences, Billerica, Massachusetts), used to prepare plasma by centrifugation at 1500g for 10 min at 4 °C and then frozen at −80 °C until analysis.

Isolation of EVs from Plasma. Plasma samples were thawed on ice and centrifuged at 3000g for 15 min at room temperature to remove cells and debris. Aliquots (250 μL) were treated with thrombin plasma prep (TEMEXO-1; System Biosciences, Inc.) for defibrination according to the manufacturer's guidelines. The clarified supernatant was transferred to a new tube and mixed with ExoQuick Exosome Precipitation Solution (EXOQ5A-1, System Biosciences, Inc.) at a 1:5 dilution, followed by a 30-min incubation at room temperature. This method induces clustering of anionic EVs with a cationic polymer, which then allows the complexes to be recovered by mild centrifugation at 1500g for 30 min at 4 °C.[32] After centrifugation, the supernatant was carefully aspirated and then the EV:polymer clusters were resuspended in a small volume of phosphate-buffered saline (PBS) for downstream analyses.

Evaluation of Size Distribution and Concentration of EVs Using Nanoparticle Tracking Analysis. Nanoparticle tracking analysis (NTA) was performed using the NanoSight NS300 instrument (Malvern Panalytical Ltd., Malvern, UK) according to the manufacturer's user manual (NanoSight NS300 User Manual, MAN0541-01-EN-00, 2017). Data capture was conducted by using NanoSight Software NTA3.2. The camera setting was adjusted to level 12 to ensure clear particle visibility without signal saturation with a screen gain of 10 and a detection threshold of 5 to include the majority of visible particles while excluding indistinct ones. Samples were diluted in PBS to a final volume of 1 mL, with concentrations adjusted to yield ranging from 30 to 200 particles per frame. PBS served as a background measurement, recording about 3 particles per frame (range of 1−5 particles per frame). To avoid contamination from previous samples, 300 μL of the sample was run at a higher speed through the system before NTA data were recorded for each analysis. Measurements consisted of recording three sequential 30 s videos at 25 frames per second (fps) with a recording cell temperature of 25 °C and a syringe speed of 100 μL/s. EVs were identified by using a 488 nm (blue) laser and an sCMOS camera. Data generated from the software included mean size, mode (predominant size population of EVs), 10th, 50th, and 90th deciles, and particle concentration (particles/mL).

UHPLC-MS/MS Analyses. EVs were resuspended in 30 mM ammonium acetate buffer (pH 7) before extraction. EV samples were then mixed with equal volume of acetonitrile/methanol (90:10; v/v), incubated for 30 min, and then centrifuged at 18,000 × g for 30 min to precipitate proteins. The supernatants containing EVs were air-dried and then reconstituted in 50% aqueous acetonitrile. UHPLC-MS/MS analyses for BDF, BDL, and DFC were performed as described[18] using a Shimadzu Nexera LC-30AD UHPLC system interfaced with a Shimadzu 8050 triple quadrupole mass spectrometer. A Waters Acquity BEH C_{18} column (2.1 × 50 mm, 1.7 μm) was used for UHPLC separations, with a mobile phase gradient from water (A) to acetonitrile (B), both

https://doi.org/10.1021/acsomega.4c10887
ACS Omega 2025, 10, 16410−16418

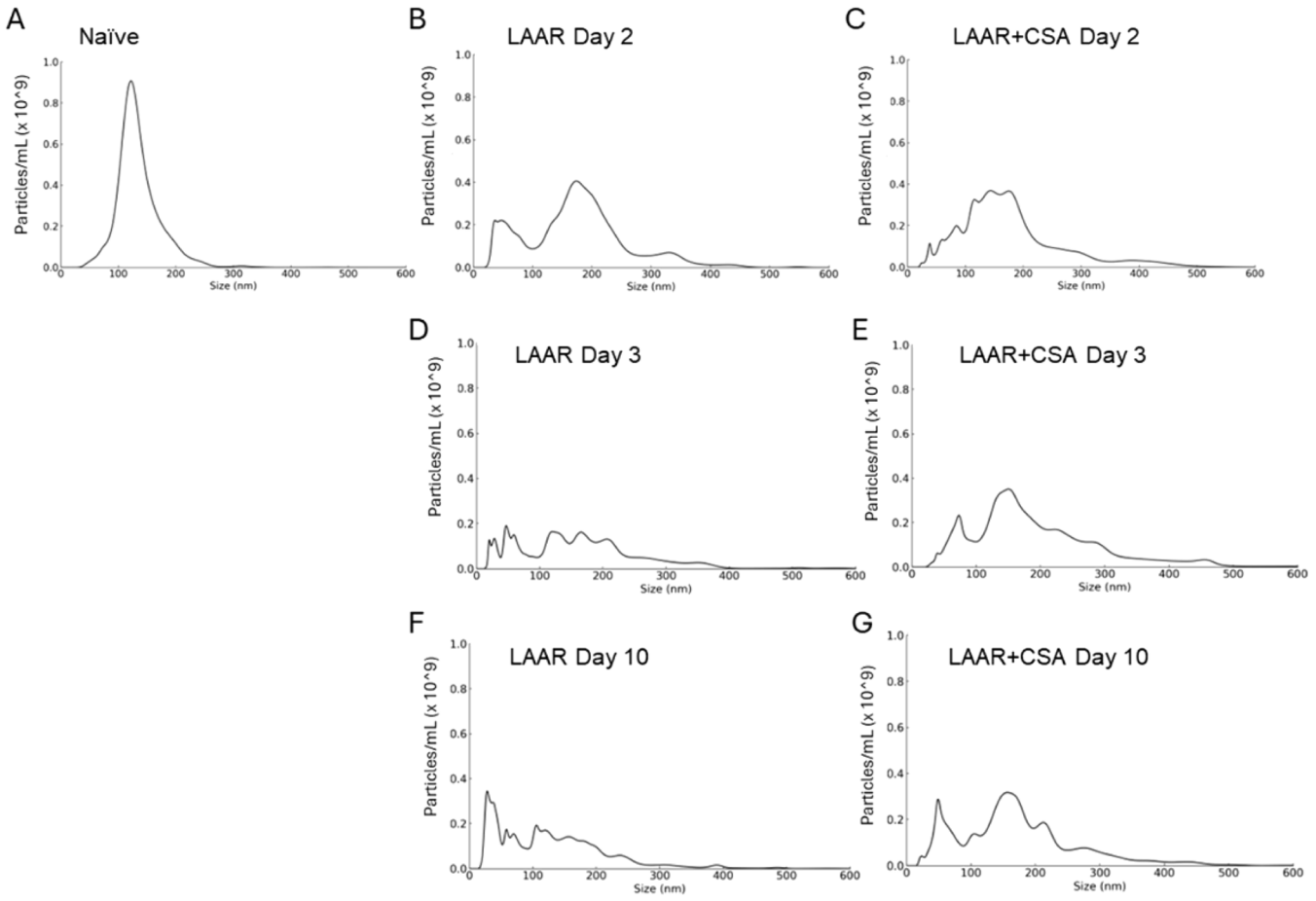

Figure 1. Exposure to LAARs alters plasma EV concentration and size distribution. NTA was carried out on EVs isolated from rabbit plasma at (A) Day 0 (naive); (B,D,F) at the indicated days after administration of LAARs; and (C,E,G) from rabbits administered LAARs and then treated with CSA beginning 1 day later. Mean EV particle concentrations were determined from 3 samples per group and are plotted against particle size.

containing 0.01% formic acid as follows: 0−0.5 min 60%−71% B, 0.5−2.0 min 71%−72% B, 2−3 min 72%−75% B, and 3−3.9 min 75%−80% B. The column was reconditioned in 60% acetonitrile for 1 min between injections. The flow rate was 0.6 mL/min, and the column temperature was maintained at 50 °C. Negative ion electrospray was used for ionization, and selected reaction monitoring tandem mass spectrometry was used for quantitative analysis.

Ex Vivo Mixing Experiment. A stock solution of BDF was prepared at a concentration of 3 mg/mL in ethyl acetate and then 10 μL diluted 1:1000 in 100% DMSO. One μL of diluted BDF (3 ng) was added to 600 μL of naive plasma for a final concentration of 5 ng/mL. The plasma mixture was then divided into three 200 μL aliquots, incubated at room temperature for up to 24 h, and then EVs were isolated as above. The BDF concentrations in plasma and EVs were then quantified by UHPLC-MS/MS.

Microglial Cell Preparation and Treatment with EVs. EVs were isolated from control, LAAR-treated, and LAARand CSA-treated rabbit plasma as above. Primary microglial cells were isolated from mixed glial cultures as previously described.[33] In brief, cerebral cortices from postnatal day 1 C57BL/6 mouse pups were cleaned of meninges, mechanically dissociated, and then placed into poly-D-lysine-coated T75 flasks in DMEM medium, supplemented with 10% fetal bovine serum (F0926, Sigma-Aldrich), and maintained at 37 °C in a humidified atmosphere with 5% CO_2. After 2 weeks when the underlying astrocytes reached confluency, microglia were dislodged by vigorous shaking, collected by centrifugation (3000 × g for 10 min), then seeded into 96-well plates at a density of 20,000 cells per well in 100 μL DMEM/F12 media, and allowed to adhere for 24 h prior to treatment. EVs derived from 150 μL total plasma (combined from 50 μL aliquots of 3 individual rabbits) in each experimental group were pooled together, resuspended in 100 μL DMEM/F12 media, diluted 4-fold in DMEM/F12 media, and then 20 μL were added to cells. After 24 h, cell death was determined as the ratio of lactate dehydrogenase (LDH) in the supernatant to total LDH measured after cells were lysed (CytoTox 96, Promega) according to manufacturer's instructions.

Data and Statistical Analysis. The effects of LAARs on EV parameters (total particles per mL, 10%, 50%, and 90% deciles; means and modes) over time were analyzed by 2-way ANOVA, followed by Sidak's multiple comparisons tests for pairwise comparisons. Cell death results were compared by 1-way ANOVA and Tukey's multiple comparison tests. Data analysis was carried out with Python-based software packages and GraphPad Prism 9.0 (GraphPad Software, San Diego, CA). At least three independent biological replicates were carried out for each experiment, and p-values <0.05 were considered statistically significant.

https://doi.org/10.1021/acsomega.4c10887
ACS Omega 2025, 10, 16410−16418

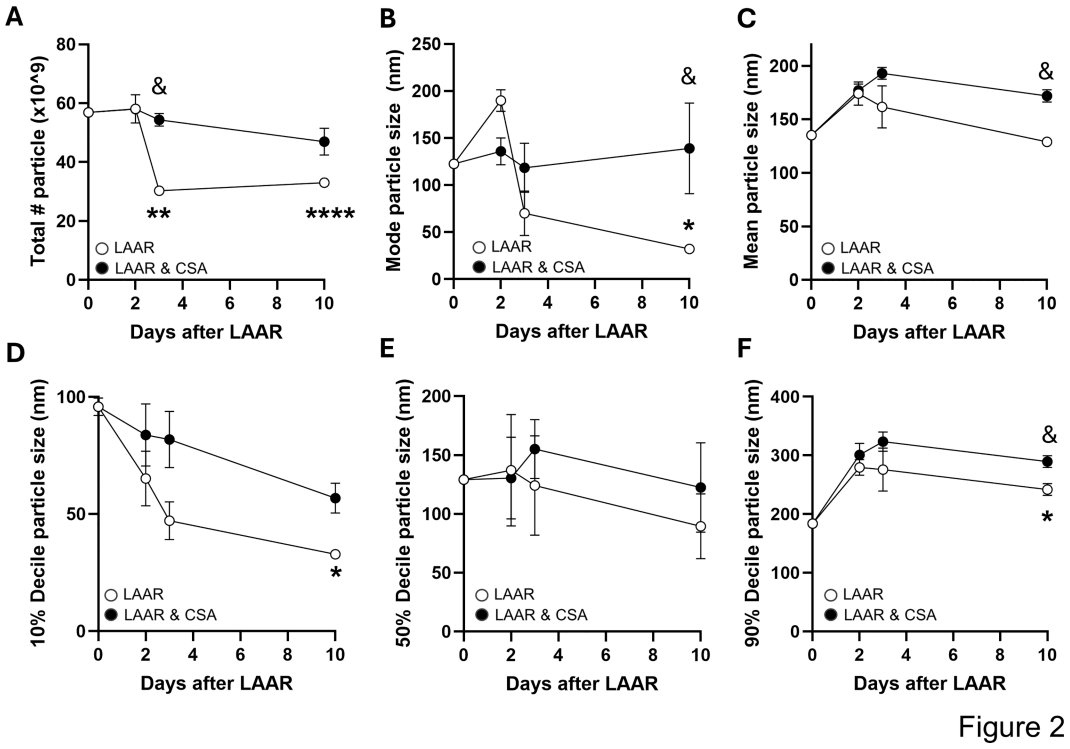

Figure 2

Figure 2. Effects of LAARs and CSA on EV particle features. NTA data from samples described in Figure 1 were analyzed for (A) total particles per mL of plasma, (B) mode, (C) mean size, (D) 10th decile, (E) 50th decile, and (F) 90th decile. Data are mean ± SE, $n = 3$ per group. *$p < 0.05$; **$p < 0.005$; ****$p < 0.0001$ compared to controls; $p < 0.05$ versus same-day BDF; 2-way ANOVA with Sidak's multiple comparisons test.

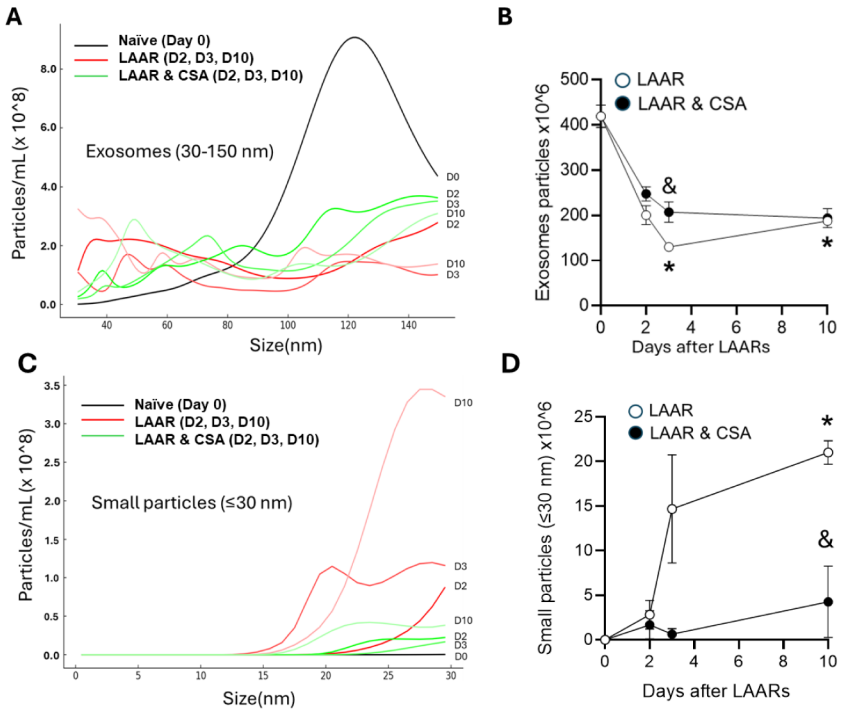

Figure 3. Effects of LAARs and CSA on exosomes and smaller particles. NTA data from samples as described in Figure 1 were analyzed for changes in the EV subpopulation concentration. The average size distribution of (A) exosomes (30−150 nm) and (C) particles sized 15 to 30 nm are shown for EVs isolated from naive (day 0, black line), LAAR days 2, 3, and 10 (red lines), and LAAR & CSA days 2, 3, and 10 (green lines). Data were then used to calculate (B, D) average concentrations over time of exposure to LAARs with or without CSA cotreatment. Data are mean ± SE, $n = 3$ per group. *$p < 0.05$ versus day 0; $p < 0.05$ versus LAAR & CSA on the same day; 1-way ANOVA with Tukey's multiple comparisons test.

https://doi.org/10.1021/acsomega.4c10887
ACS Omega 2025, 10, 16410−16418

Table 1. LAAR Concentrations in Isolated EVs

	Treatment	Sample	BDF	BDL	DFC
LAAR, ng/mL	LAAR	Plasma	622.5	1135.4	49.7
	LAAR & CSA	Plasma	412.5	609.6	34.0
	LAAR	EV	142.5	178.3	12.4
	LAAR & CSA	EV	49.1	46.0	3.0
Ratio	LAAR & CSA: LAAR	Plasma	66%	54%	69%
	LAAR	EV:Plasma	23%	16%	25%
	LAAR & CSA	EV:Plasma	12%	8%	9%
	LAAR & CSA: LAAR	EV	34%	26%	24%
Ex vivo control	BDF	Plasma	3.5 ± 1.1 (mean ± SD)		
		EV	0.2 ± 0.3 (mean ± SD)		

RESULTS

Effects of LAARs on EV Concentration and Size. Extracellular vesicles were isolated from plasma collected from adult male NZW rabbits at different times following the administration of a single bolus of LAARs. EV analyses for particle size and distribution using NTA (Figure 1) show that LAARs led to significant alterations in EV size distribution. Compared to the naive samples (Figure 1A) at 2 days after LAARs were administered, there was a noticeable shift to larger sizes as well as the appearance of a subpopulation having sizes less than 100 nm (Figure 1B). At 3 days after LAARs, a shift to larger sizes was still present, and there was an increase in the overall heterogeneity of the size distribution (Figure 1D). By 10 days after LAARs were given, the overall size distribution was similar to that observed at 3 days; however, the relative EV concentrations tended to increase in the lower size range compared to the larger size range (Figure 1F). On all days, the administration of CSA tended to minimize the effects of BDF. After 2 days (Figure 1C), the increase in concentration of smaller EVs was mostly absent, although larger EVs were still present. After both 3 and 10 days, CSA tended to reduce the overall size heterogeneity induced by BDF (Figure 1E,G), although EVs of smaller sizes were still present.

The EV size distribution was quantified by determining the mean, mode, and 10th, 50th, and 90th deciles (Figure 2). Quantification was done for EVs isolated from LAAR-treated NZWs, as well as from rabbits administered BDF and then treated with CSA beginning 1 day after LAARs. Compared to naive plasma, the average EV concentration in the LAAR-treated animals was significantly lower after 3 and 10 days (Figure 2A), and those reductions were absent in samples isolated from CSA- treated animals. Similarly, the mode was lower than controls at 3 days and significantly reduced at 10 days (Figure 2B), but it remained at control values in the CSA samples. In contrast to mode, the overall mean size was not significantly different across days (Figure 2C) although at day 10 it was higher in the CSA compared to the LAAR-only samples. The lower mode values compared to mean values reflect a greater proportion of smaller-sized particles, as suggested by histograms. Decile analysis (Figure 2D−F) is consistent with a greater proportion of smaller particles. Between days 2 and 10, there was a gradual decrease in the average size in the 10% decile, e.g., the average size of all particles that account for the lowest 10% of particles, and was significantly different from controls at day 10. The average size of the 50% decile tended to decrease over time, but those reductions were not significant. The average particle size for the 90% decile showed an increase over time that was significantly different versus controls at day 10.

LAARs Alter Exosome and Supermere Size Distribution. Since different types of EVs exhibit distinct size distributions, we analyzed the NTA data to determine whether LAARs selectively influenced a specific size distribution. Among the EV subgroups, the most notable difference was observed in the exosome size range 30−150 nm (Figure 3A). In naive samples, the exosomes showed a smooth size distribution centered near 120 nm. Treatment with LAARs for 2, 3, or 10 days greatly reduced particle concentration across this size range (Figure 3B) with maximum concentrations observed at near 120 nm. Treatment with LAARs for 2, 3, or 10 days greatly reduced exosome concentrations and led to a heterogeneous distribution of size. Treatment with CSA partially reversed the effects of LAARs, with the largest increase seen at day 3 and day 10.

In addition, treatment with LAARs increased the concentration of smaller particles (Figure 3C). Compared to naive samples, LAARs led to a time- dependent increase in particles in the 15−30 nm size range, and these increases were largely prevented by treatment with CSA (Figure 3D).

LAARs are Associated with EVs. To test whether LAARs are associated with EVs, UHPLC-MS/MS was used to quantify LAAR levels in EVs isolated from plasma 2 days after LAARs were administered and from rabbits administered LAARs and treated with CSA beginning 1 day after LAARs. Aliquots of EVs from 3 different animals were combined to provide sufficient material to measure LAAR levels over background values (Table 1). On day 2, all 3 LAARs (BDF, BDL, and DFC) were detected in EVs. Compared to the plasma from which they were isolated, levels of *cis*- and *trans*-BDF were 20−25%; BDL was 16%; and *cis*- and *trans*-DFC were 24% and 27%, respectively. Treatment with CSA for 1 day reduced all plasma LAAR levels between 31% (for *cis*-BDF) and 46% (for BDL), except for *trans*-DFC, which was modestly decreased by 7%. Reductions were also observed in EVs isolated from the CSA-treated animals, although those relative decreases were, on average, about 2-fold greater than decreases due to CSA in plasma levels. In an ex vivo control study, in which we added BDF (the most hydrophobic of the 3 LAARs) directly to naive rabbit plasma, BDF levels in the isolated EVs averaged 6% of plasma levels (Table 1). These data confirm the ability of CSA to accelerate LAAR clearance from plasma and demonstrate that LAARs are associated with isolated EVs and that association is also reduced by CSA.

EVs Derived from LAAR-Treated Rabbits Induce Microglial Cell Death. We tested whether EVs had cytotoxic effects using primary mouse microglial cells (Figure 4). After 24 h with media only, there was a background degree of cell death amounting to approximately 15%, which was reduced

https://doi.org/10.1021/acsomega.4c10887
ACS Omega 2025, 10, 16410−16418

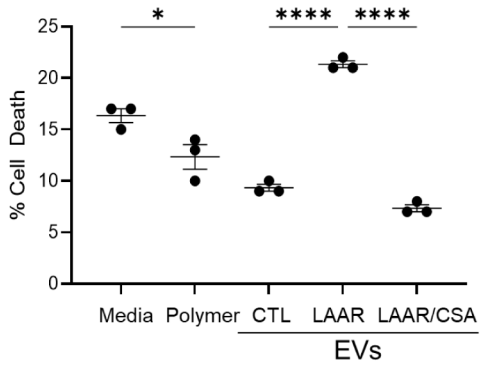

Figure 4. EVs from LAAR-treated rabbits induce microglial cell death. Primary mouse microglial cells were incubated with EVs isolated from naive plasma (EV CTL), LAAR plasma (EV LAAR), or LAAR & CSA plasma (EV LAAR & CSA). After 24 h, cell death was determined as LDH released divided by total LDH after cells were lysed. Controls included microglia incubated with DMEM/F12 media only ("media") and microglia incubated with an equivalent amount of the polymer used to precipitate EVs ("polymer"). Data are mean ± SE of $n = 3$ per group. *$p < 0.05$; ****$p < 0.0001$; 1-way ANOVA followed by Tukey's multiple comparisons test.

when the cells were incubated with the polymer used to precipitate the EVs. Incubation with EVs prepared from naive rabbits did not cause any cell death compared to the polymer alone. In contrast, incubation with EVs prepared from LAAR-treated rabbits significantly increased cell death and that increase was absent when EVs from LAAR & CSA-treated rabbits were used. These results are consistent with the lower levels of LAARs found associated with EVs from LAAR & CSA-treated rabbits. The direct addition of EVs to the LDH assay reaction did not affect absorbance readings, confirming that the effects of LAAR-EVs on microglial death were not due to alteration in assay conditions.

DISCUSSION

We show for the first time that the properties of EVs isolated from the plasma of adult rabbits exposed to potent LAARs are distinct from those isolated from naive rabbits. As soon as 2 days after LAARs were administered, there was a reduction in total EV concentration, decreasing to about 50% of the control values on days 3 and 10. At the same time, both the mean and mode particle size decreased, indicating a shift to smaller-sized EVs. The smaller average particle size is also reflected by a reduction in 10% decile. Our analysis of EV subgroups revealed a pronounced difference within the exosome size range (30–150 nm), consistent with established exosome sizes (Figure 2A).[34−36] This finding suggests that LAARs may selectively reduce exosome production, potentially affecting EV-mediated cellular communication.

In contrast to exosomes, we found that LAAR increased the concentration of smaller-sized particles in the range of 15 to 30 nm (Figure 3). These may correspond to recently described supermeres—small nanoparticles within the 1−30 nm range. Using an asymmetric-flow field-flow fractionation method, 2 subpopulations of exosomes were initially identified as well as small nonmembranous particles called exomeres, which are about 35 nm.[37] Subsequently, the same authors described the presence of smaller particles which they termed supermeres since they were found in the high-speed supernatant of the exomere preparation.[38] Initial characterization showed that supermeres are enriched in proteins and miRNAs associated with cancers, neurodegenerative diseases, and cardiovascular diseases, and they have a distinct set of snRNAs and miRNAs compared to other EV populations. Supermeres have been shown to increase lactate production from target cells, to be able to transfer drug resistance, and to cross the blood−brain barrier and accumulate in the CNS.[38] Our data therefore suggest that systemic toxicity, in this case due to anticoagulants, can increase supermere levels, which could serve as a surrogate biomarker for LAAR poisoning and provide an additional means of transporting information throughout the body. The protocol we used to isolate EVs is based on precipitation of anionic EVs clustered with a cationic polymer; a method that can also allow precipitation of smaller particles that share similar surface properties. However, it is possible that smaller particles are not precipitated with the same efficiency as larger particles; if so, we may be underestimating supermere levels. It is also possible that a portion of the smaller particles comprised aggregates of LAARs together with fragments of larger EVs; a fuller characterization is therefore required to distinguish between these possibilities.

The decreases due to LAARs observed in total particle numbers on days 3 and 10, and of particle size, mean, mode, and 10% and 90% deciles on day 10, were reduced in the EVs isolated from rabbits cotreated with CSA. Similarly, the increase in the population of smaller particles (Figure 3) was almost absent in the CSA-treated samples. Since CSA accelerates LAAR clearance from the body,[18] this may simply reflect lower LAAR concentrations. However, it is possible that CSA itself could lead to modification of the EV properties, for example, by reducing serum cholesterol levels, which are a component of EV membranes and have been shown to influence EV biogenesis,[39,40] structure,[41] and fusion.[42] Such changes could conceivably counteract the effects of LAARs on the EV properties. Further studies to evaluate the possible effects of CSA are therefore required to address this possibility.

How LAARs can influence EV properties remains to be determined. Under toxic conditions, exosome biogenesis can be affected by numerous pathways, including autophagy, which prioritizes the degradation of damaged organelles, potentially diverting resources from normal multivesicular body (MVB) formation and exosome production.[43] Our findings indicate that LAAR toxicity significantly reduces exosome numbers, which may be due to a combination of cellular stress responses, reduced energy production, altered membrane dynamics, and increased apoptosis. Toxic agents can activate stress pathways such as oxidative stress and endoplasmic reticulum (ER) stress, leading to mitochondrial dysfunction, which in turn can trigger the release of proapoptotic factors, thereby activating caspases and promoting apoptosis. Consequently, cellular resources shift toward damage repair, deprioritizing normal functions like MVB formation and exosome biogenesis.[44] LAAR-induced mitochondrial impairment[21] could therefore cause ATP depletion, triggering opening of the mitochondrial permeability transition pore, and cause further energy loss. As ATP levels decline, vesicle trafficking and MVB fusion with the plasma membrane are disrupted, resulting in diminished exosome release.[45,46] Moreover, LAAR toxicity can alter cell membrane fluidity and integrity,[21] as occurs in response to other xenobiotics.[47] Such alterations can promote the activation of proapoptotic proteins, leading to cell death,[48] thereby impeding the docking and fusion of MVBs with the plasma membrane, and reducing exosome exocytosis. It is also possible that changes in EV numbers and size distribution could be due,

https://doi.org/10.1021/acsomega.4c10887
ACS Omega 2025, 10, 16410−16418

in part, to direct membrane disruption upon interaction of LAARs with the EVs, as mentioned above for the appearance of the smaller EVs, particularly since it is known that LAARs can directly disrupt cellular membranes.[21]

The LAARs used in this study are second-generation derivatives of warfarin[12]; for this reason, they are often referred to as superwarfarins. Warfarin has previously been shown to influence EV production, thereby increasing release from vascular smooth muscle cells.[49] Since warfarin induces oxidative stress in cells, and oxidative stress is known to induce EV secretion,[50] together the data suggest that warfarin-induced oxidative stress leads to EV release. VK antagonists including warfarin can induce oxidative stress due to suppression of VK synthesis,[51] likely due to reductions of VK hydroquinone levels, a potent antioxidant that normally inhibits NADPH-dependent lipid peroxidation.[52] Additionally, both VK1 and VK2 protect against oxidative stress in primary oligodendrocytes and immature neurons[53] by inhibiting the activation of 12-lipoxygenase.[54] These findings suggest that by reducing VK levels, LAARs could increase oxidative stress and thereby modify EV secretion. However, we observed that overall EV concentrations were decreased by LAARs, although the smaller populations were increased. Since LAARs exert both anticoagulant-independent as well as VK-independent actions, it is possible that these alternative actions are the primary cause of overall reductions in EV concentration.

Our UHPLC-MS/MS analysis demonstrated that LAARs are associated with EVs. At 2 days following the administration of LAARs, plasma BDF levels were 623 ng/mL, BDL was 1135 ng/mL, and DFC was about 50 ng/mL; and these levels were reduced to between 54% and 69% when rabbits were given CSA for 1 day, consistent with previous findings.[18] Analysis of EVs isolated from the above plasma samples revealed the presence of all 3 LAARs, amounting to between 16% and 25% of respective plasma concentrations. Since plasma EV levels are estimated to be 6 orders of magnitude less than that of total lipoprotein particles,[55] the high percentage of LAARs associated with EVs argues against a nonspecific association of hydrophobic LAARs with lipophilic particles. This is supported by results of the ex vivo control experiment showing that after 1 day of incubation, only 6% of BDF in the plasma was found to be associated with isolated EVs (Table 1), compared to about 20% in EVs isolated from LAAR-treated rabbits. This experiment was carried out using a lower concentration of BDF (5 ng/mL) than that present in rabbit plasma (about 600 ng/mL) to minimize exposure of the EVs to solvents (ethyl acetate, DMSO) used to prepare BDF for the ex vivo study, solvents which could disrupt EV membranes. This is not a concern during in vivo experiments since the LAAR stock solutions are diluted 30-fold or more in corn oil and then introduced into the rabbit gut by gavage, which will further dilute the solutions as much as 50-fold. However, further experiments using higher BDF (or other LAAR) concentrations and longer incubation periods are warranted to confirm that BDF does not accumulate in EVs over time.

In all cases, LAAR levels in the EVs were reduced to between 24% and 34% in samples from CSA-treated animals, a larger reduction than observed in plasma LAAR concentrations. Further studies are needed to determine if the larger CSA-dependent reductions in EV-associated LAARs reflect selective actions of CSA on EVs; or are due to a reduction in LAAR:EV interactions due to the reduced plasma levels. It also remains to be determined if the LAARs are internalized within or bound to the external membrane of the EVs, as well as if certain size classes are more enriched than others.

Additionally, our in vitro findings show that LAAR-treated EVs induce significantly higher microglial cell death compared with both control and CSA-treated EVs (Figure 4). This increase could be due to exposure of the microglial cells to EV-associated LAARs, consistent with previous reports that LAARs can directly induce cell death in neural cells.[21] If so, the reduced cell death observed using EVs isolated from LAAR & CSA-treated samples could reflect the CSA-induced decrease in EV-associated LAARs. It is also possible that LAARs alter EV cargo or surface properties, either of which could increase EV cytotoxicity. Future studies will examine EVs isolated from LAAR-treated rabbits to characterize potential changes in their cargo.

Together, the findings of this study demonstrate that LAARs influence EV properties, potentially altering their systemic effects. Findings that LAARs are associated with plasma EVs suggest a mechanism by which EVs could facilitate LAAR distribution throughout the body, including transport across the blood–brain barrier and entry into the CNS. This may account, in part, for observation of LAAR tissue damage independent of anticoagulant actions. Findings that cotreatment of rabbits with CSA, which reduces plasma LAAR levels, also mitigated the effects of LAARs on EVs, as well as reduced EV-associated LAARs and their cytotoxicity could offer a therapeutic strategy to counter the impact of these environmental toxicants on humans.

AUTHOR INFORMATION

Corresponding Author

Douglas L. Feinstein − *Department of Anesthesiology, University of Illinois College of Medicine, Chicago, Illinois 60612, United States; Research & Development Service, Jesse Brown VA Medical Center, Chicago, Illinois 60612, United States;* orcid.org/0000-0003-2815-2885; Email: dlfeins@uic.edu

Authors

Intakhar Ahmad − *Department of Anesthesiology, University of Illinois College of Medicine, Chicago, Illinois 60612, United States; Research & Development Service, Jesse Brown VA Medical Center, Chicago, Illinois 60612, United States*

Ruth N. Muchiri − *Department of Pharmaceutical Sciences, Linus Pauling Institute, Oregon State University, Corvallis, Oregon 97331, United States*

Richard B. van Breemen − *Department of Pharmaceutical Sciences, Linus Pauling Institute, Oregon State University, Corvallis, Oregon 97331, United States;* orcid.org/0000-0003-2016-0063

Israel Rubinstein − *Research & Development Service, Jesse Brown VA Medical Center, Chicago, Illinois 60612, United States; Department of Medicine, University of Illinois College of Medicine, Chicago, Illinois 60612, United States*

Matthew Lindeblad − *Department of Pharmacology, University of Illinois College of Medicine, Chicago, Illinois 60612, United States*

Complete contact information is available at: https://pubs.acs.org/10.1021/acsomega.4c10887

https://doi.org/10.1021/acsomega.4c10887
ACS Omega 2025, 10, 16410−16418

Funding

This work was funded by NIH grant 1U01NS127746-03 (to D.L.F., R.B.v.B., M.L., I.R.) and VA BLR&D Research Career Scientist Award 5IK6BX004852-03 (to D.L.F.).

Notes

The authors declare no competing financial interest.

■ ACKNOWLEDGMENTS

The views expressed in this article are those of the authors and do not necessarily reflect the position or policy of the Department of Veterans Affairs or the United States Government.

■ REFERENCES

(1) Yoon, Y. J.; Kim, O. Y.; Gho, Y. S. Extracellular vesicles as emerging intercellular communicasomes. *BMB Rep.* **2014**, *47* (10), 531−539.
(2) Pedrioli, G.; Paganetti, P. Hijacking Endocytosis and Autophagy in Extracellular Vesicle Communication: Where the Inside Meets the Outside. *Front. Cell Dev. Biol.* **2021**, *8*, 595515.
(3) Rajendran, L.; Bali, J.; Barr, M. M.; Court, F. A.; Krämer-Albers, E. M.; Picou, F.; Raposo, G.; van der Vos, K. E.; van Niel, G.; Wang, J.; Breakefield, X. O. Emerging roles of extracellular vesicles in the nervous system. *J. Neurosci.* **2014**, *34* (46), 15482−15489.
(4) Xu, L.; Liang, Y.; Xu, X.; Xia, J.; Wen, C.; Zhang, P.; Duan, L. Blood cell-derived extracellular vesicles: Diagnostic biomarkers and smart delivery systems. *Bioengineered* **2021**, *12* (1), 7929−7940.
(5) Jayasinghe, M. K.; Pirisinu, M.; Yang, Y.; Peng, B.; Pham, T. T.; Lee, C. Y.; Tan, M.; Vu, L. T.; Dang, X. T.; Pham, T. C.; Chen, H.; Leung, A. Y. H.; Cho, W. C.; Shi, J.; Le, M. T. Surface-engineered extracellular vesicles for targeted delivery of therapeutic RNAs and peptides for cancer therapy. *Theranostics* **2022**, *12* (7), 3288−3315.
(6) Fabbri, A.; Cori, S.; Zanetti, C.; Guidotti, M.; Sargiacomo, M.; Loizzo, S.; Fiorentini, C. Cell-to-cell propagation of the bacterial toxin CNF1 via extracellular vesicles: Potential impact on the therapeutic use of the toxin. *Toxins* **2015**, *7* (11), 4610−4621.
(7) Zou, C.; Zhang, Y.; Liu, H.; Wu, Y.; Zhou, X. Extracellular Vesicles: Recent Insights Into the Interaction Between Host and Pathogenic Bacteria. *Front. Immunol.* **2022**, *13*, 840550.
(8) Pin, C.; David, L.; Oswald, E. Modulation of Autophagy and Cell Death by Bacterial Outer-Membrane Vesicles. *Toxins* **2023**, *15* (8), 502.
(9) Coelho, C.; Brown, L.; Maryam, M.; Vij, R.; Smith, D. F. Q.; Burnet, M. C.; Kyle, J. E.; Heyman, H. M.; Ramirez, J.; Prados-Rosales, R.; Lauvau, G.; Nakayasu, E. S.; Brady, N. R.; Hamacher-Brady, A.; Coppens, I.; Casadevall, A. Listeria monocytogenes virulence factors, including listeriolysin O, are secreted in biologically active extracellular vesicles. *J. Biol. Chem.* **2019**, *294* (4), 1202−1217.
(10) Dutton, R. J.; Wayman, A.; Wei, J. R.; Rubin, E. J.; Beckwith, J.; Boyd, D. Inhibition of bacterial disulfide bond formation by the anticoagulant warfarin. *Proc. Natl. Acad. Sci. U. S. A.* **2010**, *107* (1), 297−301.
(11) King, N.; Tran, M.-H. Long-Acting Anticoagulant Rodenticide (Superwarfarin) Poisoning: A Review of Its Historical Development, Epidemiology, and Clinical Management. *Transfus. Med. Rev.* **2015**, *29* (4), 250−258.
(12) Feinstein, D. L.; Akpa, B. S.; Ayee, M. A.; Boullerne, A. I.; Braun, D.; Brodsky, S. V.; Gidalevitz, D.; Hauck, Z.; Kalinin, S.; Kowal, K.; Kuzmenko, I.; Lis, K.; Marangoni, N.; Martynowycz, M. W.; Rubinstein, I.; van Breemen, R.; Ware, K.; Weinberg, G. The emerging threat of superwarfarins: History, detection, mechanisms, and countermeasures. *Ann. N. Y. Acad. Sci.* **2016**, *1374* (1), 111−122.
(13) Poessel, S. A.; Breck, S. W.; Fox, K. A.; Gese, E. M. Anticoagulant rodenticide exposure and toxicosis in coyotes (Canis latrans) in the Denver Metropolitan Area. *J. Wildl. Dis.* **2015**, *51* (1), 265−268.
(14) Fisher, P.; Campbell, K. J.; Howald, G. R.; Warburton, B. Anticoagulant Rodenticides, Islands and Animal Welfare Accountancy. *Animals* **2019**, *9* (11), 919.
(15) Gómez-Canela, C.; Barata, C.; Lacorte, S. Occurrence, elimination, and risk of anticoagulant rodenticides and drugs during wastewater treatment. *Environ. Sci. Pollut. Res. Int.* **2014**, *21* (11), 7194−7203.
(16) Acosta-Dacal, A.; Rial-Berriel, C.; Díaz-Díaz, R.; Bernal-Suárez, M. d. M.; Zumbado, M.; Henríquez-Hernández, L. A.; Luzardo, O. P. An Easy Procedure to Quantify Anticoagulant Rodenticides and Pharmaceutical Active Compounds in Soils. *Toxics* **2021**, *9*, 83.
(17) Lindeblad, M.; Lyubimov, A.; van Breemen, R.; Gierszal, K.; Weinberg, G.; Rubinstein, I.; Feinstein, D. L. The Bile Sequestrant Cholestyramine Increases Survival in a Rabbit Model of Brodifacoum Poisoning. *Toxicol. Sci.* **2018**, *165* (2), 389−395.
(18) Muchiri, R. N.; Rocha, J.; Tandon, A.; Chen, Y. L.; Alemani, R.; Ahmad, I.; McDonald, Z.; Lindeblad, M.; Rubinstein, I.; van Breemen, R. B.; Feinstein, D. L. Short-term treatment with cholestyramine increases long-acting anticoagulant rodenticide clearance from rabbits without affecting plasma vitamin K1 levels or blood coagulation. *Toxicol. Sci.* **2024**, *200* (1), 137−145.
(19) Ware, K. M.; Feinstein, D. L.; Rubinstein, I.; Weinberg, G.; Rovin, B. H.; Hebert, L.; Muni, N.; Cianciolo, R. E.; Satoskar, A. A.; Nadasdy, T.; Brodsky, S. V. Brodifacoum induces early hemoglobinuria and late hematuria in rats: Novel rapid biomarkers of poisoning. *Am. J. Nephrol.* **2015**, *41* (4−5), 392−399.
(20) Kalinin, S.; Marangoni, N.; Kowal, K.; Dey, A.; Lis, K.; Brodsky, S.; van Breemen, R.; Hauck, Z.; Ripper, R.; Rubinstein, I.; Weinberg, G.; Feinstein, D. L. The Long-Lasting Rodenticide Brodifacoum Induces Neuropathology in Adult Male Rats. *Toxicol. Sci.* **2017**, *159* (1), 224−237.
(21) Marangoni, M. N.; Martynowycz, M. W.; Kuzmenko, I.; Braun, D.; Polak, P. E.; Weinberg, G.; Rubinstein, I.; Gidalevitz, D.; Feinstein, D. L. Membrane Cholesterol Modulates Superwarfarin Toxicity. *Biophys. J.* **2016**, *110* (8), 1777−1788.
(22) Weiss, L.; Uhrig, W.; Kelliher, S.; Szklanna, P. B.; Prendiville, T.; Comer, S. P.; Edebiri, O.; Egan, K.; Lennon, Á.; Kevane, B.; et al. Proteomic analysis of extracellular vesicle cargoes mirror the cardioprotective effects of rivaroxaban in patients with venous thromboembolism Nonvalvular atrial fibrillation patients anticoagulated with rivaroxaban compared with warfarin exhibit reduced circulating extracellular vesicles with attenuated pro-inflammatory protein signatures. *Proteomics: Clin. Appl.* **2024**, *18* (4), No. e202300014.
(23) Weiss, L.; Keaney, J.; Szklanna, P. B.; Prendiville, T.; Uhrig, W.; Wynne, K.; Kelliher, S.; Ewins, K.; Comer, S. P.; Egan, K.; et al. Nonvalvular atrial fibrillation patients anticoagulated with rivaroxaban compared with warfarin exhibit reduced circulating extracellular vesicles with attenuated pro-inflammatory protein signatures. *J. Thromb. Haemostasis* **2021**, *19* (10), 2583−2595.
(24) Lami, V.; Nieri, D.; Pagnini, M.; Gattini, M.; Donati, C.; De Santis, M.; Cipriano, A.; Bazzan, E.; Sbrana, A.; Celi, A. Circulating Extracellular Vesicle-Associated Tissue Factor in Cancer Patients with and without Venous Thromboembolism. *Biomolecules* **2025**, *15* (1), 83.
(25) Hu, Y.; Repa, A.; Lisman, T.; Yerlikaya-Schatten, G.; Hau, C.; Pabinger, I.; Ay, C.; Nieuwland, R.; Thaler, J. Extracellular vesicles from amniotic fluid, milk, saliva, and urine expose complexes of tissue factor and activated factor VII. *J. Thromb. Haemostasis* **2022**, *20* (10), 2306−2312.
(26) Bonifay, A.; Cointe, S.; Plantureux, L.; Lacroix, R.; Dignat-George, F. Update on Tissue Factor Detection in Blood in 2024: A Narrative Review. *Hamostaseologie* **2024**, *44* (5), 368−376.
(27) Yang, B.; Long, Y.; Zhang, A.; Wang, H.; Chen, Z.; Li, Q. Procoagulant Properties of Mesenchymal Stem Cells and Extracellular Vesicles: A Novel Aspect of Thrombosis Pathogenesis. *Stem Cells* **2024**, *42* (2), 98−106.

https://doi.org/10.1021/acsomega.4c10887
ACS Omega 2025, 10, 16410−16418

(28) Majumder, R. Phosphatidylserine Regulation of Coagulation Proteins Factor IXa and Factor VIIIa. *J. Membr. Biol.* **2022**, *255* (6), 733−737.
(29) Borgovan, T.; Crawford, L.; Nwizu, C.; Quesenberry, P. Stem cells and extracellular vesicles: Biological regulators of physiology and disease. *Am. J. Physiol.: Cell Physiol.* **2019**, *317* (2), C155−C166.
(30) Vandenbroucke, V.; Bousquet-Melou, A.; De Backer, P.; Croubels, S. Pharmacokinetics of eight anticoagulant rodenticides in mice after single oral administration. *J. Vet. Pharmacol. Ther.* **2008**, *31* (5), 437−445.
(31) Tomlin, C. D. S. *The Pesticide Manual - World Compendium*, 15th ed.; The British Crop Protection Council: Surrey, UK, 2009.
(32) Kim, J.; Lee, H.; Park, K.; Shin, S. Rapid and Efficient Isolation of Exosomes by Clustering and Scattering. *J. Clin. Med.* **2020**, *9*, 650.
(33) Kalinin, S.; González-Prieto, M.; Scheiblich, H.; Lisi, L.; Kusumo, H.; Heneka, M. T.; Madrigal, J. L. M.; Pandey, S. C.; Feinstein, D. L. Transcriptome analysis of alcohol-treated microglia reveals downregulation of beta amyloid phagocytosis. *J. Neuroinflammation* **2018**, *15* (1), 141.
(34) Möller, A.; Lobb, R. J. The evolving translational potential of small extracellular vesicles in cancer. *Nat. Rev. Cancer* **2020**, *20* (12), 697−709.
(35) Kibria, G.; Ramos, E. K.; Lee, K. E.; Bedoyan, S.; Huang, S.; Samaeekia, R.; Athman, J. J.; Harding, C. V.; Lötvall, J.; Harris, L.; et al. A rapid, automated surface protein profiling of single circulating exosomes in human blood. *Sci. Rep.* **2016**, *6*, 36502.
(36) Doyle, L. M.; Wang, M. Z. Overview of Extracellular Vesicles, Their Origin, Composition, Purpose, and Methods for Exosome Isolation and Analysis. *Cells* **2019**, *8* (7), 727.
(37) Zhang, H.; Freitas, D.; Kim, H. S.; Fabijanic, K.; Li, Z.; Chen, H.; Mark, M. T.; Molina, H.; Martin, A. B.; Bojmar, L.; Fang, J.; Rampersaud, S.; Hoshino, A.; Matei, I.; Kenific, C. M.; Nakajima, M.; Mutvei, A. P.; Sansone, P.; Buehring, W.; Wang, H.; Jimenez, J. P.; Cohen-Gould, L.; Paknejad, N.; Brendel, M.; Manova-Todorova, K.; Magalhães, A.; Ferreira, J. A.; Osório, H.; Silva, A. M.; Massey, A.; Cubillos-Ruiz, J. R.; Galletti, G.; Giannakakou, P.; Cuervo, A. M.; Blenis, J.; Schwartz, R.; Brady, M. S.; Peinado, H.; Bromberg, J.; Matsui, H.; Reis, C. A.; Lyden, D. Identification of distinct nanoparticles and subsets of extracellular vesicles by asymmetric flow field-flow fractionation. *Nat. Cell Biol.* **2018**, *20* (3), 332−343.
(38) Zhang, Q.; Jeppesen, D. K.; Higginbotham, J. N.; Graves-Deal, R.; Trinh, V. Q.; Ramirez, M. A.; Sohn, Y.; Neininger, A. C.; Taneja, N.; McKinley, E. T.; Niitsu, H.; Cao, Z.; Evans, R.; Glass, S. E.; Ray, K. C.; Fissell, W. H.; Hill, S.; Rose, K. L.; Huh, W. J.; Washington, M. K.; Ayers, G. D.; Burnette, D. T.; Sharma, S.; Rome, L. H.; Franklin, J. L.; Lee, Y. A.; Liu, Q.; Coffey, R. J. Supermeres are functional extracellular nanoparticles replete with disease biomarkers and therapeutic targets. *Nat. Cell Biol.* **2021**, *23* (12), 1240−1254.
(39) Rodrigues-Junior, D. M.; Tsirigoti, C.; Psatha, K.; Kletsas, D.; Aivaliotis, M.; Heldin, C.-H.; Moustakas, A. TGF-β induces cholesterol accumulation to regulate the secretion of tumor-derived extracellular vesicles. *J. Exp. Clin. Cancer Res.* **2025**, *44* (1), 42.
(40) Sekhavati, N.; Noori, E.; Abbasifard, M.; Butler, A. E.; Sahebkar, A. How statin drugs affect exosomes? *J. Cell. Biochem.* **2023**, *124* (2), 171−180.
(41) Yaeger, J. D. W.; Sengupta, S.; Walz, A. L.; Morita, M.; Morgan, T. K.; Vermeer, P. D.; Francis, K. R. Cholesterol deficiency directs autophagy-dependent secretion of extracellular vesicles. *bioRXiv*. **2025**.
(42) Zhuo, Y.; Luo, Z.; Zhu, Z.; Wang, J.; Li, X.; Zhang, Z.; Guo, C.; Wang, B.; Nie, D.; Gan, Y.; Hu, G.; Yu, M. Direct cytosolic delivery of siRNA via cell membrane fusion using cholesterol-enriched exosomes. *Nat. Nanotechnol.* **2024**, *19* (12), 1858−1868.
(43) Sharma, A. Mitochondrial cargo export in exosomes: Possible pathways and implication in disease biology. *J. Cell. Physiol.* **2023**, *238* (4), 687−697.
(44) Kanamaru, Y.; Sekine, S.; Ichijo, H.; Takeda, K. The phosphorylation-dependent regulation of mitochondrial proteins in stress responses. *J. Signal Transduction* **2012**, *2012*, 931215.
(45) Tiwari, B. S.; Belenghi, B.; Levine, A. Oxidative stress increased respiration and generation of reactive oxygen species, resulting in ATP depletion, opening of mitochondrial permeability transition, and programmed cell death. *Plant Physiol.* **2002**, *128* (4), 1271−1281.
(46) Chen, Q.; Gong, B.; Almasan, A. Distinct stages of cytochrome c release from mitochondria: Evidence for a feedback amplification loop linking caspase activation to mitochondrial dysfunction in genotoxic stress induced apoptosis. *Cell Death Differ.* **2000**, *7* (2), 227−233.
(47) Tekpli, X.; Rissel, M.; Huc, L.; Catheline, D.; Sergent, O.; Rioux, V.; Legrand, P.; Holme, J. A.; Dimanche-Boitrel, M. T.; Lagadic-Gossmann, D. Membrane remodeling, an early event in benzo[a]pyrene-induced apoptosis. *Toxicol. Appl. Pharmacol.* **2010**, *243* (1), 68−76.
(48) Dingeldein, A. P. G.; Sparrman, T.; Gröbner, G. Oxidatively stressed mitochondria-mimicking membranes: A molecular insight into their organization during apoptosis. *Biochim. Biophys. Acta, Biomembr.* **2018**, *1860* (12), 2644−2654.
(49) van Gorp, R. H.; Dijkgraaf, I.; Bröker, V.; Bauwens, M.; Leenders, P.; Jennen, D.; Dweck, M. R.; Bucerius, J.; Briedé, J. J.; van Ryn, J.; Brandenburg, V.; Mottaghy, F.; Spronk, H. M. H.; Reutelingsperger, C. P.; Schurgers, L. J. Off-target effects of oral anticoagulants - vascular effects of vitamin K antagonist and non-vitamin K antagonist oral anticoagulant dabigatran etexilate. *J. Thromb. Haemostasis* **2021**, *19* (5), 1348−1363.
(50) Furmanik, M.; van Gorp, R.; Whitehead, M.; Ahmad, S.; Bordoloi, J.; Kapustin, A.; Schurgers, L. J.; Shanahan, C. M. Endoplasmic Reticulum Stress Mediates Vascular Smooth Muscle Cell Calcification via Increased Release of Grp78 (Glucose-Regulated Protein, 78 kDa)-Loaded Extracellular Vesicles. *Arterioscler., Thromb., Vasc. Biol.* **2021**, *41* (2), 898−914.
(51) Petsophonsakul, P.; Furmanik, M.; Forsythe, R.; Dweck, M.; Schurink, G. W.; Natour, E.; Reutelingsperger, C.; Jacobs, M.; Mees, B.; Schurgers, L. Role of Vascular Smooth Muscle Cell Phenotypic Switching and Calcification in Aortic Aneurysm Formation. *Arterioscler., Thromb., Vasc. Biol.* **2019**, *39* (7), 1351−1368.
(52) Mukai, K.; Morimoto, H.; Kikuchi, S.; Nagaoka, S. Kinetic study of free-radical-scavenging action of biological hydroquinones (reduced forms of ubiquinone, vitamin K and tocopherol quinone) in solution. *Biochim. Biophys. Acta.* **1993**, *1157* (3), 313−317.
(53) Li, J.; Lin, J. C.; Wang, H.; Peterson, J. W.; Furie, B. C.; Furie, B.; Booth, S. L.; Volpe, J. J.; Rosenberg, P. A. Novel role of vitamin k in preventing oxidative injury to developing oligodendrocytes and neurons. *J. Neurosci.* **2003**, *23* (13), 5816−5826.
(54) Li, J.; Wang, H.; Rosenberg, P. A. Vitamin K prevents oxidative cell death by inhibiting activation of 12-lipoxygenase in developing oligodendrocytes. *J. Neurosci. Res.* **2009**, *87* (9), 1997−2005.
(55) Johnsen, K. B.; Gudbergsson, J. M.; Andresen, T. L.; Simonsen, J. B. What is the blood concentration of extracellular vesicles? Implications for the use of extracellular vesicles as blood-borne biomarkers of cancer. *Biochim. Biophys. Acta, Rev. Cancer* **2019**, *1871* (1), 109−116.

https://doi.org/10.1021/acsomega.4c10887
ACS Omega 2025, 10, 16410−16418